Modelling of light propagation in retinal tissue

Sonny Ramachandran*[a], Nick K. Taylor[b], Andrew McNaught[c] & Andrew R. Harvey[a]
[a]School of Engineering & Physical Sciences, Heriot Watt University, Edinburgh, EH14 4AS, UK
[b]School of Mathematical & Computer Sciences, Heriot Watt University, Edinburgh, EH14 4AS, UK
[c]Gloucestershire Royal Hospital, Trust Headquarters, 1 College Lawn, Cheltenham, GL51 7AN, UK

ABSTRACT

Techniques used in retinal imaging provide a unique method for gaining information about biological structures and processes without being invasive. Applications within the fields of medicine and clinical diagnosis provide great scope for such research. Being able to measure haemoglobin oxygenation from retinal images provides useful information in the diagnosis of conditions such as diabetic retinopathy, age-related macular degeneration and glaucoma.

We describe how existing methods have been used to gain information from retinal images. Problems of calibration and difficulties encountered in validating the various models are also discussed. Existing techniques to model multi-layered tissue, such as Monte Carlo methods and radiative transfer approaches, are explained and their respective advantages and disadvantages are highlighted.

A proposal to employ a standard fundus camera, adapted to accommodate a liquid crystal tunable filter, is presented and the characteristics required of the images are outlined. We finish with a discussion of the techniques deemed to be the most promising and how the captured images can be used to validate them.

1. INTRODUCTION

With the development of ophthalmological tools to image the tissue visible in the retina, it has been possible for clinicians to view physiological features in the eye such as the optic disc, fovea, veins and arteries. With the development of optics and advances in the type of fundus cameras used, it is now possible to view the retina with a host of different light sources and more specifically with a range of wavelengths. Figures 1.a) - f) show how different structures in the retina and underlying layers can seen as the wavelength is changed[1].

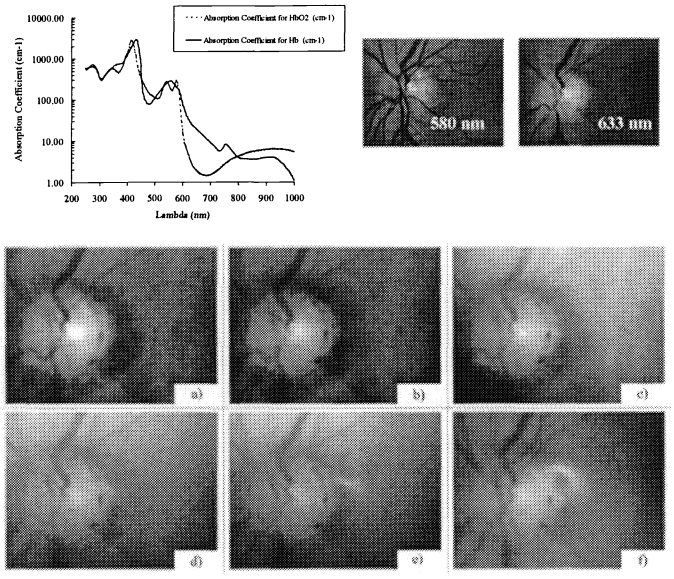

Figure 1. Plot showing the absorption coefficients for oxygenated and deoxygenated haemoglobin. Digital images of the retina taken at 580 nm and 633 nm, highlighting the sudden translucence of veins due to the dramatic drop in absorption of deoxygenated haemoglobin. Digital images **a) – f)** depicting the varying translucency of veins and arteries viewed at wavelengths 633 nm, 680 nm, 700 nm, 740 nm, 760 nm, and 800 nm respectively.

*[a] sr6@hw.ac.uk; phone +44 (0)131 451 4171; http://www.hw.ac.uk

ALT'03 International Conference on Advanced Laser Technologies: Biomedical Optics, ed. by R. K. Wang, J. C. Hebden, A. V. Priezzhev, V. V. Tuchin, Proc. of SPIE Vol. 5486 (SPIE, Bellingham, WA, 2004) · 1605-7422/04/$15 · doi: 10.1117/12.571389

It is apparent that at 633 nm arteries in the retina appear opaque and the veins appear translucent, this scenario gradually reverses as one moves through to 800 nm. Such behaviour not only gives insight into the biochemistry within obvious structures such as arteries, veins (in this case haemoglobin oxygenation) and the optic disc, but also provides some information about the tissue layers that are beneath the surface of the retina. In this way images of the retina provide a non-invasive method of gaining information about the internal structure and composition of the fundus. Structural information about the retinal and sub-retinal tissue layers can provide useful information about sight-threatening developments such as those associated with macular degeneration[2]. Loss of pigmentation and other layers (see Figure 2) characterize tissue damage that relates to vision loss.

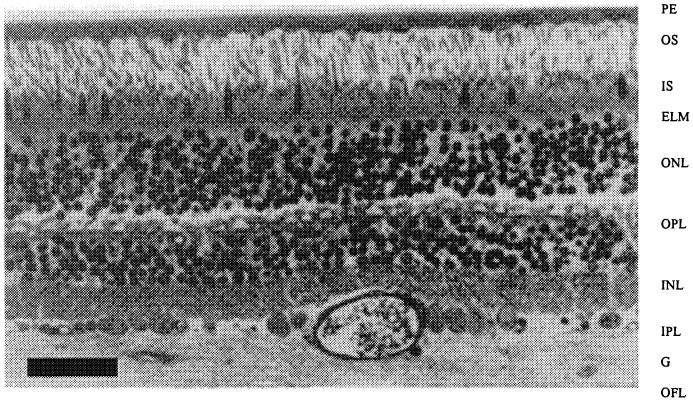

Figure 2. Light micrograph of human retina illustrates its layered structure. PE, Pigment Epithelium; OS, outer segments of photoreceptors; IS, inner segments of photoreceptors; ELM, external limiting membrane; ONL, outer nuclear layer (photoreceptor cell bodies); OPL, outer plexiform or synaptic layer; INL, inner nuclear layer; IPL, inner plexiform or synaptic layers; G, ganglion cell layer; OFL, optic fibre layer; and ILM, inner limiting membrane. Bar indicates 50 μm.

In the case of age-related macular degeneration oxidative processes give rise to radicals, which damage photoreceptor cells, retinal pigment epithelium and the choriocapillaris[3]. This also leads to the formation of debris that builds up in the Bruch's membrane, which causes it to thicken[4]. Diabetic retinopathy, which is attributed to the diabetic condition of elevated blood glucose levels, is a disorder of small blood vessels of the outer retina from which leakage of plasma occurs. Due to the leakage, lipids and lipoproteins form which can reduce the acuity of vision and can lead to blindness. It is also the most common cause of blindness in the developed world[5]. Another condition, which has the potential to seriously impair vision is glaucoma[6], where increased intraocular pressure (IOP) causes cupping of the optic disc, as well as thinning of the neuroretinal rim (see Figure 3).

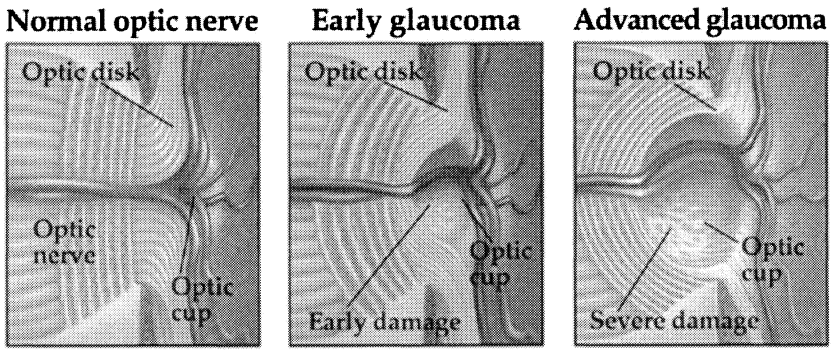

Figure 3. An outline of the progressive damage caused by the onset of glaucoma.

With all of the outlined conditions a reliable and convenient method of determining structure and composition would be of great value to clinicians, in so far as to provide early diagnosis. An example of such progress is early work carried out by DeLori on the oximetry of blood vessels, visible at certain wavelengths in the eye. In the outlined disorders, damaged tissue often results in a lack of metabolism and in the presence of veins and arteries this often leads to an anomaly in the levels of oxgenated and deoxygenated haemoglobin. Accurate measurements of such anomalies give insight into the

level of tissue damage and hence gauge the severity of a particular condition. Given that absorption spectra for oxygenated and deoxygenated blood can be accurately determined, reflectance spectra of a vein can provide oximetric measurements (see Figure 4).

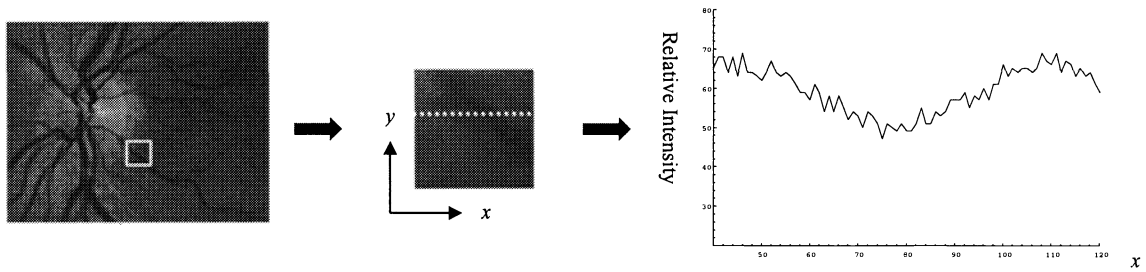

Figure 4. a) Digital image of the retina obtained at 560nm, depicting a cropping region about a vein emanating from the optic disc. b) Cropped image (128 x 128 pixels) with highlighted region about y = 80 pixels. c) Plot showing the variation in intensity along x at y = 80 pixels. Drop in intensity is attributed to absorption by blood within vein.

In this paper a number of popular models used to model light propagation in tissue, to gain structural and spectral information are put forward. The success and limitations when applied to real cases are discussed and the construction of appropriate instrumentation for gaining useful retinal images is outlined.

1. THEORETICAL APPROACHES

1.1 Kubelka-Munk theory

Kubelka-Munk theory (KMT) was originally developed to describe the properties of light reflected from paint films, but has now been applied to many different problems of light transport in turbid media. The principles are simple in that the model initially considers the effects of scattering and absorption, propagating in two opposed directions and incident upon some medium with arbitrary coefficients of scattering and absorption. Formulation of the model starts with the following set of coupled differential equations[7]:

$$-\frac{dI}{dx} = -(S+K)I + SJ \qquad \frac{dJ}{dx} = -(S+K)J + SI \tag{1}$$

where $I(x)$ and $J(x)$ are the isotropic diffuse intensities corresponding to forward and backward diffuse radiation respectievly, S and K are the effective scattering and absorption coefficients per unit length of the media and x is the distance from the non-illuminated side to the medium. By some manipulation and integration of the two differential equations one can obtain the following expression for the Kubelka-Munk diffuse reflectance:

$$R_{KM} = \frac{1 - R_g\left[a - b\coth(bSh)\right]}{a + b\coth(bSh) - R_g} \tag{2}$$

where R_g is the diffuse reflection coefficient for light incident on the media, h is the thickness of the media, $a=(S + K)/S$ and $b=(a^2-1)^{1/2}$. Figure 5. depicts the scenario dictated by the model outlined above. It is important to note that Equation (2) does not take into account the partial reflectance of incident light at the illuminated surface, nor the internal partial reflectance of diffuse light at the media-air interface. If one takes these boundary reflection effects into account then the effective diffuse reflectance becomes

$$R_{dd} = r_d^e + \frac{(1-r_d)(1-r_d^e)R_{KM}}{1 - r_d R_{KM}} \tag{3}$$

where r_d^e and r_d are the reflection coefficients for diffuse light incident on the air-media and media-air interfaces, respectively.

This approach is known as the two-flux Kubelka-Munk theory and is well described by experimental results providing the illumination is with diffuse monochromatic light, the medium is sufficiently turbid and light is scattered diffusely. The theory works best for optically thick materials where >50% of the light is reflected and <20%is transmitted[8]. For the case that the incident light is collimated a better description is given by the four-flux Kubelka-Munk approach. The approaches differ from two-flux theory in that there are two diffuse fluxes counter-propagating within the given medium as well as two collimated light beams which are incident on the medium and reflected from the rear boundary respectively. These models simply describe scattering in the forward and backward directions, a more precise description of three-dimensional scattering is given by the seven-flux Kubelka-Munk model. This is the simplest three-dimensional representation of scattered light as well as incident light in a semi-infinite medium. To achieve greater accuracy multi-flux (discrete ordinates) theory can be employed, which approximates to a solution of the transport equation (see section 2.3) by considering illumination along many discrete directions.

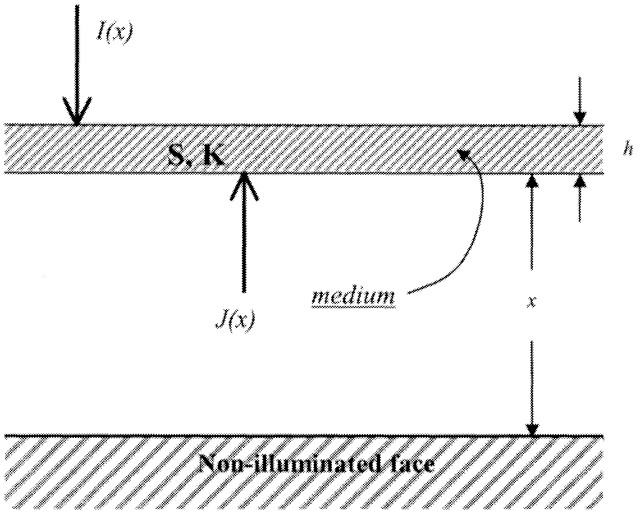

Figure 5. Diagram depicting the two-flux Kublenka-Munk model. *I(x)* and *J(x)* are the foward and backward intensities, incident upon a media, *h* thick, with scattering and absorption coefficients *S* and *K* respectively.

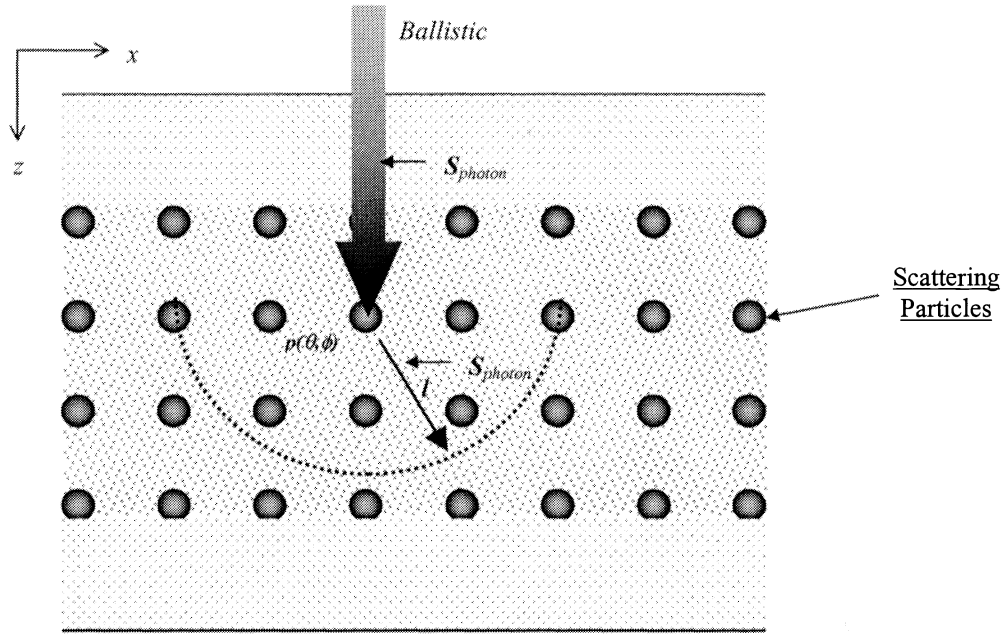

Figure 6. Diagram depicting a photon with Stokes vector S_{photon} and pathlength l, incident upon a particle with phase function $p(\theta,\phi)$.

1.2 Monte Carlo Approach

Monte Carlo techniques have been applied to fields ranging from particle to solid-state physics, but have only recently been successfully employed to describe photon migration in tissues. The basic foundation is the 'method of direct imitation simulation of photon migration in a medium'. The model works by recording the path of each single photon, contained in a given flux, as it moves through a scattering medium. Photons that pass through the medium without being scattered are often referred to as 'ballistic photons'. During the course of any given photon's path, an event can occur and such events are described with an appropriate probability distribution. In the case of simulating light propagation in tissue, photons would either be elastically scattered or absorbed through collisions with scatterers within the medium. The outcome of a given event is determined by use of a uniform random distribution of numbers. Note that the probability of a given photon being scattered in a particular direction is determined at the point where a given particle is located in the medium. For a complete account of events, it is necessary to specify the scattering cross-section and scattering matrix for every given photon-scattering particle interaction within the medium.

Suppose a single photon enters a scattering medium and is allowed to travel some pathlength l. The free pathlength l, is random quantity and takes values given by the probability density[9]

$$p(l) = \rho\sigma_{ext} \exp\left[-\rho\sigma_{ext} l\right], \tag{4}$$

where ρ is the particle concentration and σ_{ext} is the extinction cross-section. For any given photon, the value of l obtained is determined by a random number, γ, that is uniformly distributed over the interval [0,1]

$$\gamma = \int_0^l p(l)dl. \tag{5}$$

Substitution of Equation (4) into Equation (5) leads to the pathlength, given by

$$l = \left(\frac{1}{\rho\sigma_{ext}}\right)\ln|\gamma|. \tag{6}$$

If it is to happen that a particular photon traverses the distance l (thus remaining within the scattering volume), then the possible events of scattering and absorption are selected randomly. In spherical coordinates, the probability density of scattering within a specified direction is dependent on two terms; $p(\theta,\phi)$ that depends upon the scatttering particle's Mueller matrix $M(\theta,\phi)$ and the Stokes vector $\boldsymbol{S}$ associated with the photon. As the photon traverses the medium ballistically, the consecutive points are related by a sequence of transformations that depends upon the particular type of chosen coordinates. With each scattering event that takes place, the vector $\boldsymbol{S}$, is altered accordingly and a new value for $\boldsymbol{S}$ is determined. The new vector is the result of the preceding vector transformed into the new scattering plane and the Mueller matrix of the scattering particle. By use of a random number generator, the next value of l in the direction the photon is travelling is found and a new value for it's coordinates are found within the space of scattering particles.

The procedure outlined is repeated until the photon's direction is such that it is not within the boundaries of the scattering system. Within the simulation, detectors (points where the photon's attributes and history are recorded) can be placed and photon's with attributes of interest can be registered according to given parameters i.e. distance covered or the scattering multiplicity. For each emitted photon, its direction and coordinates of where it was emitted and the number of scattering events experienced are all recorded. An increase in the number of particles used in the simulation reduces statistical uncertainty and also provides greater insight into the spatial distribution of scattered light. When put into practice, such related Monte Carlo techniques correlate with relations derived from solving the transfer equation analytically (see Section 2.3).

1.3 Finite-difference Transport

A fast way of accurately describing the light distribution in large heterogeneous media is given by the finite-difference solution of the transfer equation, sometimes referred to as the discrete-ordinate formulation. Initial development of the

transfer equation is credited to Bouguer and Lambert and it was in 1950 that Chandrasekher first proposed its use to describe the transport of radiation in arbitrary media.

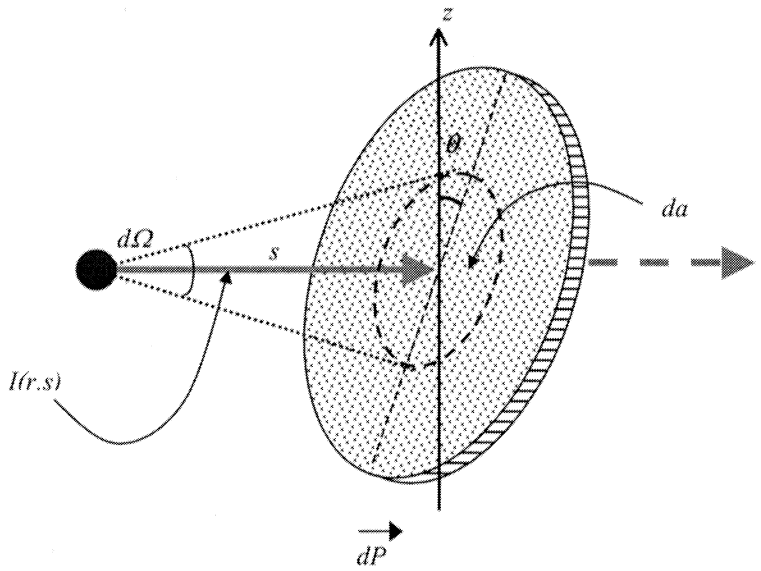

Figure 7. Incident intensity *I(r,s)* about solid angle $d\Omega$ near direction *s*, concentrated on an area *da* at an angle *6* to the z-axis, resulting in an energy flow *dP*.

It is only recently that finite-difference solutions of the transfer equation have been applied to tissue, with the only exception being Rasteger *et al* (1989) who used such a method to calculate the one-dimensional fluence rate of radiation in a small slab-like homogeneous medium. Before outlining the implementation of the finite-difference technique, a description of the transfer equation is necessary. The transfer equation is derived from energy considerations and makes use of the classical assumptions of ray optics, that there are no radiating sources within the medium as well as the statistical approximation that rays of light propagating in different directions are mutually incoherent. Suppose a ray of light has intensity $I(\underline{r},\underline{s})$ travelling with direction *s*, is incident upon a medium (orientated at an angle θ to the z-axis), resulting in a energy flow *dP* through an area *da* which is concentrated about a solid angle $d\Omega$ (near the direction *s*) in the frequency interval (ν, $\nu + d\nu$). Such a scenario is depicted in Figure 7 and is described by the relation[10]:

$$dP = I(\underline{r},\underline{s})\cos\theta da d\Omega d\upsilon . \tag{7}$$

To implement the relation in Equation (7) for radiative transfer, the Boltzman equation used in the kinetic theory of gases and in neutron transfer is applied. This results in the main stationary equation of radiative transfer theory (RTT), which for monochromatic light, has the form[11]

$$\frac{\partial I(\bar{r},\bar{s})}{\partial \bar{s}} = -\mu_t I(\bar{r},\bar{s}) + \frac{\mu_s}{4\pi}\int_{4\pi} I(\bar{r},\bar{s}')p(\bar{s},\bar{s}')d\Omega' , \tag{8}$$

where $I(\bar{r},\bar{s})$ is the radiation intensity at a point $\bar{r}$ in the direction $\bar{s}$ with the units $Wm^{-2}sr^{-1}$. The scattering phase function is given by $p(\bar{s},\bar{s}')$ and $d\Omega'$ is the unit solid angle in the direction $\bar{s}'$. Equation (8) is an integro-differential equation that describes the transfer of radiation across an infinitesimally small volume of scattering media. The integral term in Equation (8) describes the change in intensity $I(\bar{r},\bar{s})$ due to scattering along the direction *s* by considering all other directions *s'* whilst the term $\mu_t I(\bar{r},\bar{s})$ describes the attenuation of radiation due to the processes of scattering and absorption. The function $p(\bar{s},\bar{s}')$ is known as the scattering phase function, but is analogous to the scattering probability density function mentioned earlier (see Section 2.2), in that it describes the probability of a photon being scattered in the direction $\bar{s}'$ given that it is travelling in the direction $\bar{s}$. Note that if the scattering effects in the

particular medium are symmetric then the phase function depends solely upon the angle between the directions $\bar{s}$ and $\bar{s}'$. The portion of radiation that decreases due to scattering and absorption (I_{ri}) is given by,

$$\frac{\partial I_{ri}(\bar{r},\bar{s})}{\partial \bar{s}} = -\mu_t I_{ri}(\bar{r},\bar{s}). \tag{9}$$

The remaining portion is that manifesting in the medium due to scattering (I_d), which when taking into account that the total intensity (I_{total}) is the sum of both portions leads to

$$I_{total}(\bar{r},\bar{s}) = I_{ri}(\bar{r},\bar{s}) + I_d(\bar{r},\bar{s}), \tag{10}$$

where I_d is often referred to as the diffusion intensity. Since I_d is described by Equation (8), then the diffusion intensity can be written as

$$\frac{\partial I_d(\bar{r},\bar{s})}{\partial \bar{s}} = -\mu_t I_d(\bar{r},\bar{s}) + \frac{\mu_s}{4\pi}\int_{4\pi} I_d(\bar{r},\bar{s}')p(\bar{s},\bar{s}')d\Omega' + \varepsilon_{ri}(\vec{r},\vec{s}), \tag{11}$$

where $\varepsilon_{ri}(\vec{r},\vec{s})$ is the intensity required for a source that accounts for the attenuation in the incident radiation. It is of interest to observe that Equation (9) agrees with Bouguer's law that

$$I(x) = I_0 e^{-Kx}, \tag{12}$$

where I_0 is the intensity at the source, $I(x)$ is the attenuated intensity at some distance x and K is the extinction coefficient. Note that effects that are deviations from Bouguer's law, such as 'darkening' and 'clearing' due to the dense packing of scattering particles are hence not accounted for within transfer theory.

For non-trivial media, the transfer equation is not analytically soluble and satisfactory solutions require numerical approaches to the finite-difference expression of the transfer equation. The goal of any such algorithm is to find $I(\bar{r},\bar{s})$ or to determine the energy fluence-rate, which is expressed in the units Wm^{-2}. In order to use a finite-difference approach, the angular (Ω) and spatial (r) variables need to be distcretised. The method outlined here is that put forward by Hielscher *et al* (1998). Spatial discretisation is achieved by the Crank-Nicolson method (Alcouffe 1993, Press *et al* 1992), whilst angular discretisation is achieved by the method of discrete ordinates (Carlson and Lathrop 1968, Bell and Glasstone 1970). The technique involves dividing the radiation field into a series of discrete directions (Ω_m). Instead of there being a single integro-differential equation, a transformation results in there being a set of coupled integro-differential equations. Each of these equations is then transformed into a linear differential equation, by expanding the phase function, p, into a series of Legendre polynomials P_l, such that[12]

$$p = \sum_{l=0}^{L} \frac{(2l+1)}{4\pi} b_l P_l, \tag{13}$$

where b_l is the corresponding expansion coefficient. With iteration of the algorithm new values for the fluence-rate are generated until the solution converges. To aid reaching a solution the diffusion approximation to the transfer equation (see Section 2.4) can be used as a measure of the speed at which convergence is occurring (analogous to the 'Verlet-velocity' method employed in algorithms used to solve similar systems of differential equations). Since desirable solutions of the finite-difference transfer equation require algorithms that have to be tackled numerically, such methods are constrained by the limitations of computational resources.

1.4 Diffusion Theory

When photons are propagating in a medium there reaches a point where the optical path is such that the scattered light is broadened and can be considered isotropic (it appears to have 'forgotten' its initial direction of propagation). In such a

situation it is simpler to approximate the isotropic radiation to some appropriate approximation of the transfer equation. Supposing the transfer equation (Equation (11)) is given in the form described by Hielscher *et al* (1998),

$$\Omega \cdot \nabla \Psi(r,\Omega) + (\mu_a(r) + \mu_s(r))\Psi(r,\Omega) = S(r,\Omega) + \int_{4\pi} \Psi(r,\Omega') p(\Omega \cdot \Omega') d\Omega' \ , \tag{14}$$

where

$r \equiv$ Position vector

$\Omega \equiv$ Unit vector pointing along direction of propagation

$\Psi(r,\Omega) \equiv$ Energy radiance in untits $\mathrm{Wcm^{-2}sr^{-1}}$

$S(r,\Omega) \equiv$ Power injected into a solid angle centred on Ω in a unit volume at r (Source term)

$\mu_a \equiv$ Absorption coefficient

$\mu_s \equiv$ Scattering coefficient

$p(\Omega \cdot \Omega) \equiv$ Phase function .

Diffusion theory is based upon an approximation of the transfer equation, derived from expanding Ψ into spehrical harmonics and only considering the first two terms. Case and Zweifel (1967) show that the energy radiance can be written as

$$\Psi(r,\Omega) = \frac{1}{4}\int_{4\pi} \Psi(r,\Omega) d\Omega + \frac{3}{4}\pi \Omega J(r), \tag{15}$$

where *J(r)* is correction term. By inserting Equation (15) into Equation (14) a series of manipulations leads to the diffusion equation

$$-\nabla(3\mu_a + 3\mu_s')^{-1}\nabla\Phi(r) + \mu_a\Phi(r) = S(r). \tag{16}$$

Note that μ_s has been replaced by μ_s', which is defined in terms of the anistropy factor, g, where

$$\mu_s' = \mu_s\left[1 - \int_{4\pi} \Omega' \cdot \Omega p(\Omega' \cdot \Omega) d\Omega'\right] \quad \& \quad g := \int_{4\pi} \Omega' \cdot \Omega p(\Omega' \cdot \Omega) d\Omega' . \tag{17}$$

When considering a physical explanation, the inverse of μ_s' is regarded as the distance a photon has to travel before it loses information about its direction (often referred to as the reduced or transport mean free path). For now it is assumed that the diffusion coefficient, D, takes the form

$$D = (3\mu_a + 3\mu_s')^{-1}, \tag{18}$$

although alternate definitions have been proposed such as $D = (3\mu_s')^{-1}$ (Furutsu and Yamada 1994) and $D = (\mu_a + 3\mu_s')^{-1}$ (Wang and Jacques 1995). Unlike transfer theory, for simple geometries analytic solutions can be found such as in an infinite medium that contains an isotropic point source, with intensity $I_0(W)$, at r_0 one can express the fluence-rate, $\Phi(r,t)$, as

$$\Phi(r,t) = \frac{I_0}{4\pi D}\frac{\exp\left[-(\mu_a/D)^{1/2}|r - r_0|\right]}{|r - r_0|} . \tag{19}$$

Diffusion theory is a simpler model to that proposed by solving the transfer equation and proves a valid check for finite-difference transfer calculations but has its limitations (see Section 3.1).

1.5 Other approaches

The approaches outlined so far are ones, which have been popular to implement as well as give rise to useful information – but there are other techniques. Optical tomography in the near infrared has been used to image the structure of human tissue and works on the basis that by analysing the time taken by photons to traverse a medium, structural information can be determined. The principle is that photons traversing a medium will have a range of different pathlengths, which is attributed to the scattering and absorbing properties. Analysis of the distribution of times taken and hence the pathlengths provides a description of the properties of the medium. The technique has been widely used, but for non-trivial types of heterogeneous tissue the method becomes considerably complex. A novel approach is that outlined by Random-walk theory (RWT), which describes the statistical behaviour of random walks, constrained along a finite number of discrete directions. It has been shown that for photon migration in homogeneous media, the theory agrees with results obtained from numerical solutions of the transfer equation (Bonner *et al* 1987, Gandjbakhche and Weiss 1995). Unfortunately due to its complexity, the theory has only been successfully applied to model only simple media. With similar success is the Markov random field method, which was developed by Grünbaum *et al*. The model is based upon describing transport events in terms of their respective transition probabilities, but has never been applied to realistic scenarios. Relating to the background theory outlined in Section 1.3, is the Finite element method (FEM). The technique is more complicated, than those employed in finite difference solutions of the transfer equation (FDM), but it proves effective for describing non-trivial geometries and complex boundary effects. Analogous to FDM, the starting point is the transfer equation, but where the method differs is that it approximates the solution to a finite number of basis functions that exist within a vector space. This then reduces the problem to an algebraic matrix, which is resolved using well-known algorithms. As with the prior methods, the technique becomes considerably complex and descriptions of non-trivial media becomes increasingly difficult. The final technique to merit discussion in this section, is the possibility for improvement by considerations of the perturbation amplitudes in the time domain[13]. For any given equation describing transport properties, a description of the sensitivity of time- or frequency- domain measurements of transmitted light to localised perturbations of the optical properties within the medium can be provided. A number of investigations have incorporated perturbations into the diffusion equation, whilst Gandjbakjche *et al* have performed similar analysis to RWT. The method is a useful addition to current approaches and provides a route to quantify accuracy as well as test validity when comparing results to those obtained experimentally.

2. CURRENT APPLICATIONS

2.1 Simulation in various media

Numerous applications of the approaches outlined (see Section 1) to model light propagation have been carried out, but in this section only a few, relating to the most popular techniques are discussed. Kubelka-Munk theory has been used for an extensive period by those working in the paint industry to characterize the absorbing and scattering properties of polymer coatings. Much work surrounds the generation of simple layered models, which include partial and boundary reflections so that inversion techniques can determine the optical parameters from given reflectance spectra[14]. An extension of this model, not only considers scattering in the forward and backward directions, but also considers lateral scattering. The method proves valuable when describing the optical properties of halftone prints on paper[15]. More complex applications have been exploited by Claridge *et al*. A multi-layered model is assumed to describe the skin and associated properties of absorption and scattering are included from experimental results. Within the simulation emitted light is characterized by the definition of three separate colours (red, green and blue), such that a colour space representing the contributions from each layer is obtained. Studies were carried across different ethnic groups, so that for any given person parametric maps for particular layers in the skin could be obtained[16]. Unlike Kubelka-Munk theory, finite-difference solutions of the transfer equation have had far more extensive applications. Studies carried out by Guo *et al*, examine the influence of inhomogeneities in a homogeneous medium and extend their models to try and explain imaging anomalies found in the human head, such as in the skull, cerebrospinal fluid (CSF), grey matter and white matter. In parallel to these studies, is comparison with results obtained from the diffusion approximation to the transfer equation[17]. Hielscher *et al* (1998) conducted a similar study, with extensive comparisons not only between finite-difference solutions and diffusion theory, but with results obtained from Monte Carlo simulations. Monte Carlo techniques are not only a method of verification but also a valid approach that has been applied to various cases. Three-dimensional MRI scans obtained of the human head have been converted into parametric maps of scattering and absorption coefficients, which have been used in simulations with detectors 1 mm^2, placed 30 mm from with 108 photons. Reasonable results were obtained with computation times of 5 – 10 hours, using a Pentium III, 1 GHz CPU[18]. Instead of using parametric maps obtained from MRI scans, Okada *et al* use Mone Carlo simulations to model the

propagation of near-infrared light in an adult human head, with the novel approach of describing the embedded particles as cylindrical scatterers[19]. The propagation of polarized light, to obtain polarised backscattered images by Jaillon *et al*[20].

2.2 Simulation in the Retina

Some of the earliest work in studying the propagation of light in the retina was presented by Delori, Norren and Tiemeijer (1989). The models proposed (often referred to as Delori models I-III) assume the anterior layers of the retina to be layered and homogeneous. Absorption and scattering within each medium is accounted for by the absorption coefficient and attenuation is consistent with Bouger's law (see Equation 12.). The distinction between models I to III is in the complexity of layers and the associated reflections at interfaces[21] (see Figure 8.).

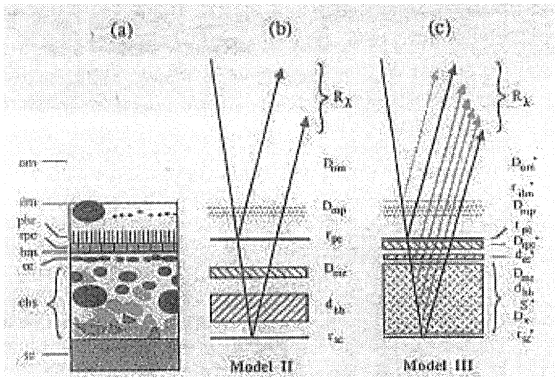

Figure 8. a) Schematic representation of the fundus layers; *om*, ocular media; *ilm*, inner limiting membrane; *phr*, photoreceptors; *rpe*, retinal pigement epithelium; *bm*, Bruch's membrane; *cc*, choriocapillaries; *chs*, choroidal stroma; and *sc*, sclera. b) and c) are diagrams for models II and III repspectively. Parameters with an asterix are fixed; the others are adjusted by curve fitting in each model. The *D* symbols represent single-pass densities, *r*, reflectances, and *d*, blood layer thickness.

The models outlined by Delori *et al*, do not aim to provide a complete description of light transport in the retina, but have provided a firm foundation for much of the work carried out in this field. In Section 2.1 work carried out by Claridge *et al*, making use of a three dimensional colour space to characterize the presence of different skin layers was outlined. Related work has now been extended to provide similar parametric maps of layers found in retinal tissue. Not only has the technique made use of variations upon Kubelka-Munk theory[22], but has also been compared with results gained from Monte Carlo simulations[23]. This work has been successful for simple layered simulations and has the potential goal to serve as an aid to clinicians diagnosing diabetic retinopathy, by indicating areas of tissue damage. Much of the accuracy when modelling light transport in the eye, is subject to the accuracy with which scattering (especially in layers

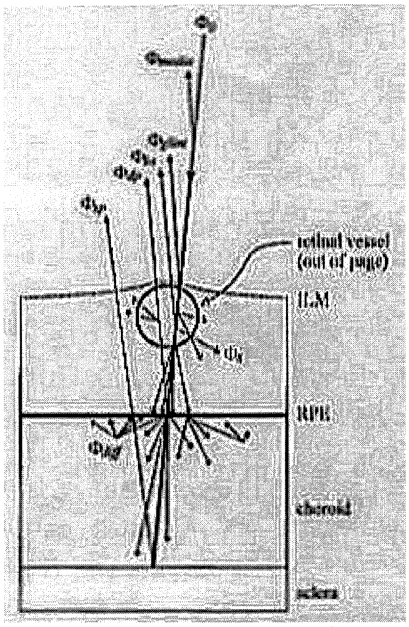

Figure 9. Primary light paths associated with a scanning-beam retinal vessel oximetry measurement; Φ_0, incident light; Φ_{media}, scattered light from the lens and vitreous; Φ_{glint}, specular reflection from the inner limiting membrane (ILM) or vessel wall; Φ_s, light scattered away by red blood cells (RBC's) within the vessel; Φ_{bs}, light backscattered to the detector by RBC's; Φ_{sp}, light collected that traversed the vessel in single pass; Φ_{dp}, light collected that has traversed the vessel in double pass; Φ_{diff}, light diffused laterally in the choroid; RPE, retinal pigment epithelium.

containing pigment) can be accounted for. A novel approach, is presented by Miura *et al*, who used a scanning confocal laser to probe the deeper sub-retinal layer (hence avoiding the pigmented layers) and optical tomography to generate a three-dimensional of the structure. The technique is successful in minimising the effects of pigment associated scattering and has the potential to be highlight areas where exudative processes associated with age-related macular degeneration might have taken place[24]. As yet the applications mentioned do not deal with the special case of a vein or artery embedded in the sub-retinal tissue, which is of particular interest for accurate sub-retinal blood oximetry. Monte Carlo simulations have been used to characterize the effects caused by the refractive index discontinuity between the red-blood cells and plasma within the vein, as well as the contribution made by photons that have made single and double passes through a vein (see Figure 9.).

Work in this particular area has shown that such effects are significant, but due to the large number of parameters required to characterize the behaviour, there have been as yet no accurate applications to retinal vessel oximetry[25]. Similar work to model such effects has also been carried by Hammer *et al*[25]. It is important to observe, that the applications mentioned in this section are just a few from a myriad of different approaches. Although Monte Carlo, Delori and Kubelka-Munk techniques have been applied to the retina, as yet solution of the transfer equation have not been widely used.

2.3 Proposition for Instrumentation

With the development of new techniques to model light propagation in the retina, comes the need to obtain viable data, with which, theoretical results can be validated and calibrated. This can be facilitated by hyperspectral imaging of the retina in which spectral images are recorded in many narrow spectral bands[26]. Installing the filter, requires intercepting the source light before it is incident upon the eye, which is achieved by having the filter unit inside the optical system of the opthalmoscope. There are several techniques with which this can be achieved. In a preliminary investigation we employed a modified conventional fundus camera in which the light source was filtered by narrow band interference filters to record spectral data cubes. Although this process was somewhat slow it demonstrated that post-detection coregistration of narrow band images is possible and also those parts of the spectrum where most useful for clinical diagnostics. In the future it will be necessary to record images much more rapidly and two techniques are being pursued; a novel two-dimensional snapshot spectral imaging technique[27] and the replacement of the manually changed interference filters with a liquid crystal tuneable filter (LCTF). This latter development is more appropriate for validating imagery since it more readily enables narrow-band imaging. The LCTF is installed so as to directly filter the light source, as shown in Figure 10. This configuration attenuates the total light intensity incident upon the eye and offers less patient discomfort than filtering the light reflected from the eye. The transmitted light intensities are somewhat lower than for a conventional fundus camera and thus a high-performance cooled camera is used. The system is interfaced to a computer for control and data acquisition and this enables automated capture of a spectral data cube, with electronic band selection and a 10 nm spectral resolution.

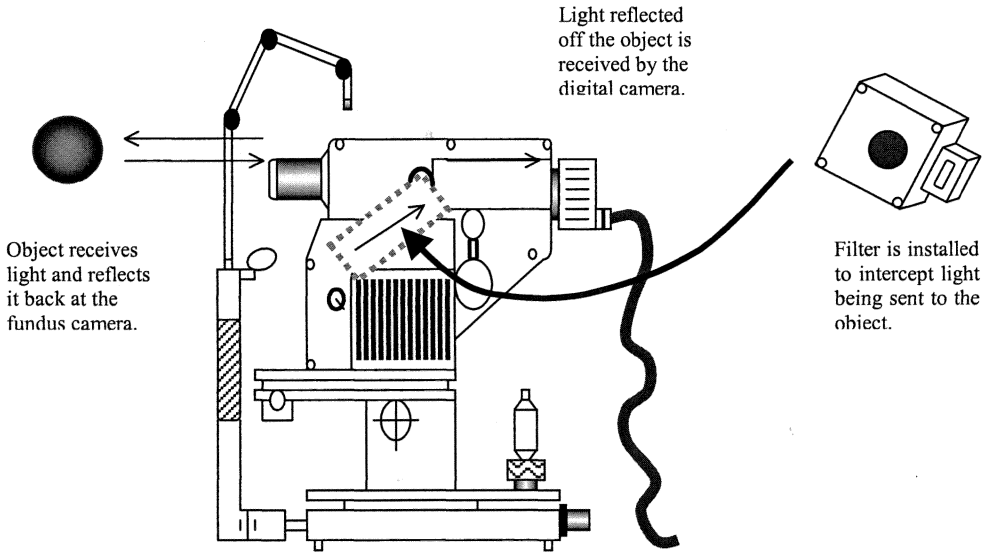

Figure 10. A depiction of how the LCTF unit is installed into the optical system of the opthalmoscope.

4. EVALUATION

So far described has been the motivation for modelling light propagation in the retina, some theory relating to popular techniques, applications and a proposition for a useful method of obtaining data. As with all approaches there are some that succeed where others fail but there are also areas which current techniques are not yet able to account for completely. Monte Carlo techniques carry the potential to offer the most complete picture of light propagation in the retina. Use of the Mueller matrix can account for effects of polarisation and utilisation of the bi-directional reflection function (BRDF) can provide a more accurate depiction of scattering within retinal tissue. Within the model is also the capacity to describe effects of non-trivial geometries such as veins, arteries and non-uniform scattering layers. With increased complexity the technique proves to be computationally expensive and is prone to statistical variations of a few percent. It can also prove impracticable to reduce these errors since computation time increases by a factor of four, when the accuracy is doubled. A faster approach is that described in finite-difference solutions of the transfer equation, which although do not provide a complete picture of light propagation in the retina, can provide useful models for investigating the effects of inhomgeneities as well provide useful insight into the physical processes occuring. Altering the scalar form of the transfer equation (see Equation 11) to describe the intensity, as a matrix, enables the theory to account for effects due to polarisation. For special cases where light propagating in the retina appears to be isotropic, diffusion approximations of the transfer equation provide a suitable description. With the approaches discussed it is often of great use to be able to invert the model, with respect to real data, to be able to obtain optical parameters defining the region. An interesting notion associated with such inversions is the concept of uniqueness. For example the variation in measured reflected intensity along a vein, embededed in tissue, may appear the same as that for a vein different embedded in tissue with different optical parameters. Such anomalies are difficult to locate and it is only through detailed analysis of a multitude of different scenarios that one can be sure that their inverted solution, is indeed an accurate depiction of reality. With all the models outlined, their true validity can only be confirmed if they agree with experimental results. With most digital images obtained of the retina, the mapped intensities are relative and it is accurate knowledge of the albedo that provides models with a route to verification. Such concerns as these are ones of calibration and there are many errors that can affect accuracy, since the optical properties of one person's eye could be significantly different from that of someone elses. The search for invariant spectral signatures within the eye, offers one route, in that features such as the optic disc or blemishes on the surface of the retina could hold useful characteristics. A real-time method of monitering the size of the pupil whilst data is being obtained can also provide calibration, providing a model describing the variation in intensity through a model eye can be constructed. It is clear from this section that there are a couple of techniques that hold promise and their implementation depends upon the nature of the information one is seeking a particular model to describe.

5. CONCLUSIONS

In this paper the motivation for studying light propagation in the retina has been outlined. Theoretical background into popular techniques as well application in various media, including the retina has been described. A useful technique of instrumentation has also been proposed to obtain high quality digital images of the retina at wavelengths in the visible spectrum has been proposed. To conclude, it is of merit to mention that due to the hard work of many researchers, light propagation in the retina is a growing field, with improvements apparent in the flux of new literature. There are still yet many problems to be solved before a satisfactory description of light transport in the retina is established, but with novel advances and useful approximations the field seems to be one, which is active.

ACKNOWLEDGMENTS

In acknowledgment of EPSRC for DTA support, Heriot-Watt University and the Cheltenham Eye Clinic.

REFERENCES

1. J. Lawlor, D. W. Fletcher-Holmes, A. I. McNaught & A. R. Harvey, "In vivo hyperspectral imaging of the human retina and optic disc". The Association for Research in Vision and Development, Anatomy and Physiology/Retinal Cell Biology. 4350-B319. Annual Meeting Fort Lauderdale, Florida, May 5-10, 2002 and A. R. Harvey, J. Lawlor, A. I. McNaught, J. W. Williams & D. W. Fletcher-Holmes. "Hyperspectral imaging for the detection of diseases". SPIE 4816-37 Conference on Imaging Spectrometry VIII, Seattle, July 7-11, 2002.

2. Masahiro Miura, "Three-dimensional imaging in age-related macular degeneration", Optics Express, Vol.9, No.9, pp. 436-443, (2001).
3. Barry S. Winkler, "Oxidative damage and age-related macular degeneration", Mol Vis, **5**, pp. 32, (1999).
4. François C. Delori *et al*, "Autofluoresence Distribution Associated with Drusen in Age-Related Macular Dengeneration", Investigative Opthamology & Visual Science, Vol.41, No.2, pp. 496-504, (2000).
5. Stephen J. Preece & Ela Claridge, "Physics based medical image understanding of the colouration of the ocular fundus with application to the detection of diabetic retinopathy", Medical Image Understanding and Analysis, pp. 7-10, (2000).
6. James E. Morgan, "Optic nerve head structure in glaucoma: astrocytes as mediators of axonal damage", Eye, **14**, pp. 437-444, (2000).
7. William E. Vargas, "Inversion methods from Kubelka-Munk analysis", J. Opt. A: Pure Appl. Opt. , **4**:452-456 (2002).
8. P. Kubelka and F. Munk. "Ein Beitrag zur Optik der Farbanstriche". Zeits. f. techn. Physik, **12**,pp. 593-601, (1931).
9. Valery V. Tuchin, "Handbook of Optical Biomedical Diagnostics", **1**, pp.116, (2002).
10. Valery V. Tuchin, "Handbook of Optical Biomedical Diagnostics", **1**, pp.110, (2002).
11. A. Ishimaru, "Wave Propagation and Scattering", Academic Press, San Diego (1969).
12. Andreas H. Hielscher *et al*, "Comparison of finite-difference transport and diffusion calculations for photon migration in homogenous and heterogeneous tissues", Phys. Med. Biol., **43**,pp.1285-1302, (1998).
13. Jeremy C. Hebden & Simon R. Arridge, "Imaging through scattering media by the use of an analytical model of perturbation amplitudes in the time domain", Applied Optics, Vol. 35, No. 34, pp. 6788-6796, (1996).
14. William E. Vargas, "Inversion methods from Kubelka-Munk analysis", J. Opt. A: Pure Appl. Opt. , **4**:452-456 (2002).
15. Safer Mourad, "Extending Kubelka-Munk's Theory with Lateral Light Scattering", International Conference on Digital Printing Technologies, Vol. 17, pp. 469-473, (2001).
16. Symon D'Oyly & Ela Claridge, "Developing a predictive model of human skin colouring", Proceedings of SPIE, Vol. 2708, pp. 814-825, (1996).
17. Zhixiong Guo & Kyunghan Kim, "Ultrafast-laser-radiation transfer in heterogeneous tissues with the discrete-ordinates method", Applied Optics, Vol. 42, No. 16, pp. 2897-2905, (2003).
18. D. A. Boas *et al*, "Three dimensional Monte Carlo code for photon migration through complex heterogeneous media including the human head", Optics Express, Vol. 10, No. 3, pp. 159-170, (2002).
19. Eiji Okada & David T. Delpy, "Near-infra-red light propagation in an adult head model. I. Modelling of low-level scattering in the cerebrospinal fluid layer", Applied Optics, Vol. 42, No. 16, pp. 2906-2914, (2003).
20. Frank Jaillon & Hervé Saint-Jalmes, "Description and time reduction of a Monte Carlo code to simulate propagation of polarized light through scattering media", Applied Optics, Vol. 42, No. 16, pp. 3290-3296, (2003).
21. François C. Delori & Kent P. Pflibsen, "Spectral reflectance of the human ocular fundus", Applied Optics, Vol. 28, No. 6, pp.1061-1077, (1989).
22. Stephen J. Preece & Ela Claridge, "Physics Based Medical Image Understanding of the Colouration of the Ocular Fundus with Application to Detection of Diabetic Retinopathy"
23. Stephen J. Preece & Ela Claridge, "Monte Carlo modelling of the spectral reflectance of the human eye", Phys. Med. Biol., **47**, pp. 2863-2877.
24. Masahiro Miura *et al*, "Three dimensional imaging in age-related macular degeneration", Optics Express, Vol. 9, No. 9, pp. 436-443, (2001).
25. Matthew H. Smith *et al*, "Effect of multiple light paths on retinal vessel oximetry", Applied Optics, Vol. 39, No. 7, pp. 1183-1193, (2000).
26. M. Hammer *et al*, "Light Paths in Retinal Vessel Oxymetry", IEEE Transactions on Biomedical Engineering, Vol. 48, No. 5, pp. 592-598, (2001).
27. J. Lawlor, D. W. Fletcher-Holmes, A. I. McNaught & A. R. Harvey, "In vivo hyperspectral imaging of the human retina and optic disc". The Association for Research in Vision and Development, Anatomy and Physiology/Retinal Cell Biology. 4350-B319. Annual Meeting Fort Lauderdale, Florida, May 5-10, 2002 and A. R. Harvey, J. Lawlor, A. I. McNaught, J. W. Williams & D. W. Fletcher-Holmes. "Hyperspectral imaging for the detection of diseases". SPIE 4816-37 Conference on Imaging Spectrometry VIII, Seattle, July 7-11, 2002.